

A Comparison of One-Shot and Recovery Methods in T1 Imaging

ADRIAN P. CRAWLEY AND R. MARK HENKELMAN

*Ontario Cancer Institute and Department of Medical Biophysics,
University of Toronto, Toronto M4X 1K9, Canada*

Received August 18, 1987

Spin-lattice (T1) relaxation times are conventionally estimated using inversion recovery or saturation recovery sequences. Such "recovery" methods are limited in magnetic resonance imaging by the long times required to collect multiple points along the T1 relaxation curve. This problem can be overcome by the use of "one-shot" methods, which collect all points along the relaxation curve in a single excitation. We have compared the relative efficiency of these methods, on the basis of the signal-to-noise ratio obtained in the calculated T1 image from an exam time of fixed duration. We have found that a one-shot method using stimulated echoes has a poor efficiency. However, a method based on a technique first proposed by Look and Locker has an efficiency that is almost equal to the inversion recovery method and therefore possesses highly favorable properties for T1 imaging.

© 1988 Academic Press, Inc.

INTRODUCTION

Multipoint T1 imaging is performed by acquiring $N \geq 3$ images corresponding to N points along the relaxation curve. Multipoint measurements enable systematic errors due to imperfect tip angles to be minimized by a three-parameter least-squares fitting procedure that explicitly models the effects of the tip angles (1-4). When N is large, a check for multiexponentiality can be performed, to reduce errors due to partial volume effects and to characterize multicompartiment relaxation curves (5).

Inversion recovery (IR) and saturation recovery (SR) techniques are conventionally used for multipoint determinations of T1 relaxation times in NMR. The use of such "recovery" methods in magnetic resonance imaging (MRI) is severely limited by long exam times. In a multipoint recovery method, considerable time is required for the partial recovery of longitudinal magnetization between the measurement of successive points along the T1 relaxation curve. For example, a 256×128 pixel image, calculated from $N = 10$ points using a repetition time $TR = 2.5$ s, requires an exam time equal to $128 \times 10 \times 2.5$ s, i.e., 53 min.

In response to this problem, the use of stimulated echoes (ST) has been proposed as a possible "one-shot" method for T1 imaging (6, 7). More recently, another one-shot method, first proposed by Look and Locker (8) for measuring T1 relaxation times in NMR, has been introduced to the MRI community (9-11). We shall refer to this as the LL method. One-shot methods use a series of limited flip angles to progressively tip longitudinal magnetization into the transverse plane, so that all points to be measured along the T1 relaxation curve are sampled on each excitation. The time required to perform the multipoint sequence can be much shorter for a one-shot method than

that for a recovery method, and the exam time is therefore kept within reasonable bounds.

The use of limited flip angles in one-shot methods inevitably causes a reduction in the signal-to-noise ratio (SNR) of the data relative to recovery methods. However, the reduced sequence time of a one-shot method allows for more signal averaging over a long exam time, which will cause a relative improvement in the SNR compared to a recovery method with the same exam time.

In this paper, we compare the various multipoint methods in terms of the SNR in a T1 image that is calculated from data acquired in a fixed exam time. The comparison essentially concerns the relative “efficiency” of the methods in acquiring data that will produce a T1 image with the maximum SNR in a given exam time. The same figure of merit has also been used by other authors for the comparison of two-point sequences in T1 imaging (12). We specifically address the question whether one-shot methods have an efficiency similar to that of the conventional recovery methods.

FIGURE OF MERIT

For the sake of clarity, we first consider the MR imager working in a “spectrometer” mode, i.e., with all the gradients turned off. We consider a multipoint T1 sequence used to measure the T1 relaxation curve of a small sample, whose size is equal to a voxel in normal “imaging” mode. We denote the signal acquired (without signal averaging) at time t along the relaxation curve by $S(t)$, and the standard deviation of the signal due to random noise by σ_0 . We define the “dynamic range” of the multipoint experiment as $DR = S(0) - S(\infty)$. The SNR of the data is given by DR/σ_0 , prior to any signal averaging. An estimate of T1 can be obtained from these data using a least-squares fitting procedure. The noise propagation of the least-squares fit can be characterized by the dimensionless factor

$$b = \frac{\sigma_{T1}/T1}{\sigma_0/DR}. \quad [1]$$

The noise factor b depends only on the times $\{t_i/T1\}$ at which the T1 relaxation curve is sampled (and in the case of the LL method on the limited flip angle). The calculation of b follows from least-squares statistics (13) and is given in the Appendix. If the multipoint sequence is repeated N_{rep} times, and the data are signal averaged, the SNR of the T1 estimate is given by

$$T1/\sigma_{T1} = (DR/\sigma_0)N_{\text{rep}}^{1/2}/b. \quad [2]$$

We now consider the MR imager in its conventional “imaging” mode. It has been shown (14, 15) that the 2DFT imaging process performs N_{pe} signal averages on each pixel signal, where N_{pe} is the number of phase encode steps. If the multipoint pulse sequence is also repeated N_{ex} times for each phase encode step, we have $N_{\text{rep}} = N_{\text{ex}}N_{\text{pe}}$. The exam time, T_{exam} , is given by $T_{\text{exam}} = N_{\text{rep}}T_{\text{seq}}$. The SNR in the calculated T1 image is therefore given by

$$\frac{T1}{\sigma_{T1}} = \frac{DR}{\sigma_0} \frac{1}{b} \left(\frac{T_{\text{exam}}}{T_{\text{seq}}} \right)^{1/2}. \quad [3]$$

We are interested in comparing the efficiency of multipoint T1 sequences in terms of the SNR of the calculated T1 image obtained in a fixed exam time. We therefore set T_{exam} and σ_0 to unity and define a relative figure of merit Γ :

$$\Gamma = \frac{\text{DR}}{bT_{\text{seq}}^{1/2}}. \quad [4]$$

The efficiency Γ therefore depends on three characteristics of the multipoint sequence. Maximizing the dynamic range (DR) improves the SNR in the data $\{S_i\}$ before signal averaging, whereas minimizing the sequence time (T_{seq}) increases the number of signal averages within a fixed exam time. The noise propagation factor b is minimized by optimizing the sampling times $\{t_i/T1\}$ (and the limited flip angle in the case of the LL method). In general terms, the recovery methods (IR and SR) have a fairly high dynamic range DR, whereas the one-shot methods (ST and LL) have a lower DR due to the use of limited flip angles. However, one-shot methods require a shorter T_{seq} to sample the T1 recovery curve. To establish which method has the highest efficiency, we must therefore investigate the balance between the competing effects of DR and T_{seq} on the SNR of the multipoint data.

PULSE SEQUENCES

In the previous section, we defined a relative figure of merit Γ (Eq. [4]) in terms of DR, T_{seq} , and b , which will enable a comparison of the relative efficiencies of the various methods. Before making such a comparison, we first optimize each method by maximizing Γ over the relevant sequence parameters. In this section, we introduce the four pulse sequences and discuss the restrictions that were applied to the choice of sequence parameters used in the optimization procedure. We also derive expressions for DR and T_{seq} for the four methods.

The pulse sequences are given in Table 1, together with expressions for their dynamic range DR and sequence time T_{seq} . The multipoint signals $\{S_i\}$ obtained with each method are illustrated in Fig. 1. The T2 dependence of the signals is given

TABLE 1
Pulse Sequences and Signal Equations for the Multipoint T1 Methods

Pulse sequence ^a	Seq. time T_{seq}	Signal equation ^b $S_i = \text{DR} \exp(-t_i/T1) + \beta$	
		DR	β
IR $\pi - t_i - \pi/2 - \text{Acq} - (\text{TR} - t_i) -$	$N \cdot \text{TR}$	-2	$1 + e^{-\text{TR}/T1}$
SR $t_i - \pi/2 - \text{Acq} -$	$N \cdot t_N/2$	-1	1
ST $\pi/2 - \pi/2 - \{\alpha_i - \text{Acq} - \tau -\}_i - W -$	$t_N + W$	$\frac{1 - e^{-W/T1}}{2N^{1/2}}$	0
LL $\pi - \{\alpha - \text{Acq} - \tau -\}_i -$	t_N	$\frac{-(1-u)}{1-uv} \left(\frac{v(1-[uv]^{N-1})}{(1+v[uv]^{N-1})} + 1 \right) \sin \alpha$	$\frac{1-u}{1-uv} \sin \alpha$

^a $t_i = (i-1)\tau$, $\{\dots\}_i$ signifies a repetition over $i = 1$ to N .

^b For the LL method, $u = e^{-\tau/T1}$, $v = \cos \alpha$, and T1 is replaced by $T1_{\text{eff}}$ (given by Eq. [10]).

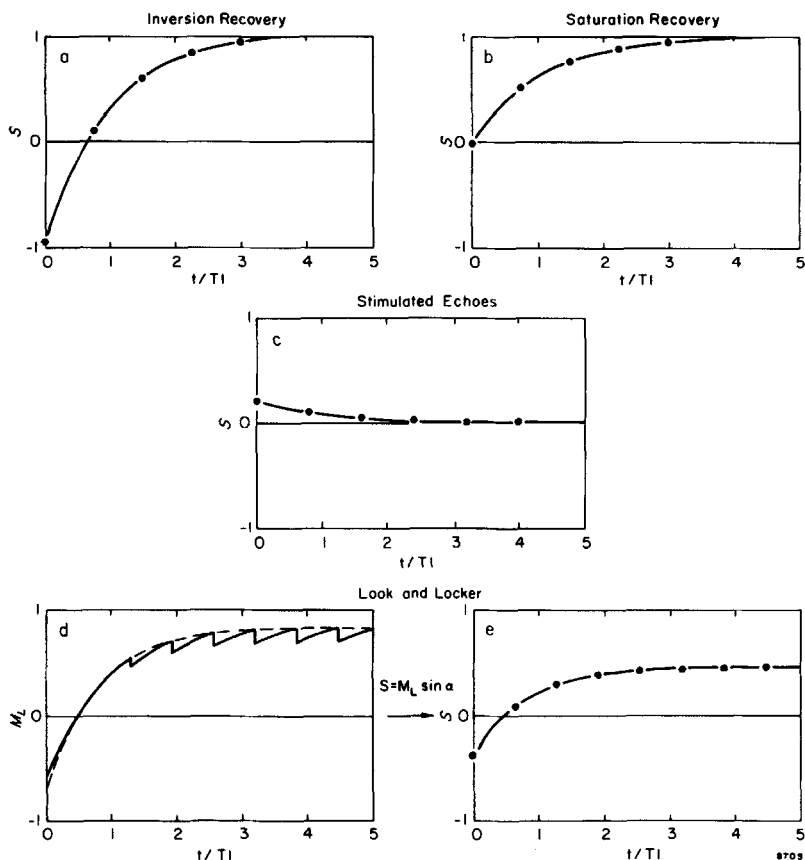


FIG. 1. Multipoint signals $\{S_i\}$ plotted as a function of time along the T_1 relaxation curve, for (a) inversion recovery, (b) saturation recovery, (c) stimulated echoes, (d-e) Look and Locker method. The signals shown are in fact those obtained from the optimized pulse sequences and are expressed in units of the fully relaxed longitudinal magnetization. The dashed curve in (d) is characterized by an effective T_1 relaxation time, given by Eq. [10].

by $\exp(-TE/T_2)$ for all four methods, where TE is the echo time, and we can therefore ignore this term in our comparison. The signals are then expressed in Table 1 and Fig. 1 in units of the equilibrium magnetization.

The conventional recovery methods require no introduction. A number of modifications to the IR method have been proposed, however, and the implementation usually found on commercial MRI units is known in the literature as the modified fast IR (MFIR) sequence (16). This modification keeps the repetition time TR constant, by varying the waiting time W_i between the 90° pulse and the next 180° pulse, so that $TR = t_i + W_i = \text{constant}$ for all i . We note that since t_N must satisfy the inequality $t_N < TR$, the full DR given in Table 1 is not achievable with a finite TR .

In the stimulated echo method (6, 7), the first two 90° pulses are used to store a part of the magnetization longitudinally. This stored magnetization decays over time according to the T_1 relaxation time. Each limited flip angle α_i samples this decay by

tipping out a small transverse component of magnetization. The resulting signals therefore provide a set of measurements along this T1 decay curve, as shown in Fig. 1c, from which T1 can be estimated. In the Look and Locker method (8), a constant limited flip angle α is applied repeatedly. The resulting signals give a measure of the approach of the longitudinal magnetization to a steady state, as shown in Figs. 1d and 1e. The approach to steady state is exponential and is characterized by an "effective" T1 relaxation time, $T_{1\text{eff}}$, which we define later. The true T1 relaxation time can be calculated from $T_{1\text{eff}}$. Using the modification proposed by Kaptein *et al.* (17), a 180° inversion pulse is applied at the beginning of the sequence, to increase the DR of the signals.

Although there can be some benefit in using a nonlinear spacing of the sampling times $\{t_i\}$ (1, 2), we restrict our analysis to linear spacing. The first sampling time t_1 is always set to zero. This has been shown to be optimal for T1 estimation using a three-parameter fit to IR data (1, 2), and it is intuitively obvious that it is an optimal choice for all of the methods considered here. Strictly, t_1 can never be precisely zero, especially in the SR and ST methods, where the minimum repetition time must be greater than the time (T_s) required to sample the data. In practice, $T_s \ll T1$ in biological tissues of interest, and we can safely ignore the effects of a finite T_s in our analysis.

The expressions for T_{seq} given in Table 1 follow immediately from the pulse sequence timings. The DR values given for the recovery methods are well known. We derive below the expressions for the DRs of the one-shot methods.

The ST method uses variable limited flip angles $\alpha_{i-1} = \arctan(\sin \alpha_i)$, with the final limited flip angle $\alpha_N = 90^\circ$, to tip equal magnetization (M_T) into the transverse plane in the absence of T1 relaxation (6, 7). Since $\alpha_N = 90^\circ$, the longitudinal magnetization at the end of the waiting time W is $M_L = (1 - \exp(-W/T1))$. Let M_{Li} be the "stored" magnetization just prior to the i th limited flip angle pulse. After application of the two 90° pulses, one-half of the magnetization is lost to a spin-echo signal, and the "stored" longitudinal magnetization is

$$M_{Li} = M_L/2 = (1 - \exp(-W/T1))/2. \quad [5]$$

In the absence of relaxation, each limited flip angle tips out a constant transverse magnetization M_T :

$$\begin{aligned} M_{L2}^2 &= M_{L1}^2 - M_T^2 \\ &\vdots \\ M_{LN}^2 &= M_{L(N-1)}^2 - M_T^2 = M_T^2. \end{aligned} \quad [6]$$

Therefore,

$$M_T = M_{L1}/N^{1/2} = (1 - \exp(-W/T1))/(2N^{1/2}). \quad [7]$$

In the presence of T1 relaxation, we have $S(0) = M_T$, and $S(\infty) = 0$. The dynamic range $DR = S(0) - S(\infty) = M_T$ is therefore given directly by Eq. [7].

A waiting time W must be included in the ST method, to allow some recovery of the longitudinal magnetization. In the LL method, however, it is the recovery of this magnetization that is actually being measured in the one-shot estimation of T1. Although the limited flip angles do not allow complete recovery of the longitudinal magnetization, we have considered a waiting time W equal to zero for the LL method.

The method of deriving the expression for the DR of the LL method is as follows. According to Look and Locker (8),

$$M_{Li} - M_L(\infty) = (M_{Li} - M_L(\infty))[uv]^{i-1} \quad [8]$$

$$M_L(\infty) = (1 - u)/(1 - uv), \quad [9]$$

where $u = \exp(-\tau/T1)$ and $v = \cos \alpha$. The magnetization M_{Li} therefore relaxes towards $M_L(\infty)$ with an effective T1 given by

$$T1_{\text{eff}} = \tau/(\tau/T1 - \ln(\cos \alpha)). \quad [10]$$

This effective T1 is always shorter than the true T1, as shown in Fig. 1d. Equations [8] and [9] assume that there is no residual transverse magnetization immediately preceding each limited flip angle pulse; i.e., we assume that either $\tau \gg T2$ or appropriate spoiler gradients are applied. We also have

$$S_i = M_{Li} \sin \alpha. \quad [11]$$

Therefore,

$$\text{DR} = (M_{Li} - M_L(\infty)) \sin \alpha. \quad [12]$$

The steady-state magnetization M_{Li} after the inversion pulse is

$$M_{Li} = -vM_{LN}. \quad [13]$$

Substituting into Eq. [8], with i equal to N , we can solve for M_{Li} . Finally, substituting M_{Li} into Eq. [12], together with $M_L(\infty)$ from Eq. [9], we obtain the expression for DR shown in Table 1.

LEAST-SQUARES FITTING

In the previous section, we derived expressions for the dynamic range DR and the sequence time T_{seq} of each method. In order to find the efficiency Γ of each method (Eq. [4]), we must calculate the noise propagation b through the least-squares fitting routine. In this section, we discuss the options available in performing a least-squares fit to the multipoint data. A detailed calculation of b is given in the Appendix.

An estimate of T1 is obtained from a set of multipoint data $\{S_i\}$ by a least-squares fitting procedure, which minimizes the error propagated into the T1 estimate from the random noise σ_0 . The fitting equation must correctly model the experimental data if systematic errors are to be avoided. Assuming monoexponential T1 behavior (i.e., neglecting partial volume effects, etc.) the multipoint data from any of the four sequences can be modeled by

$$S_i = \text{DR} \exp(-t_i/T1) + \beta, \quad [14]$$

where DR has already been introduced as the dynamic range, $\text{DR} = S(0) - S(\infty)$, $\{t_i\}$ are the sampling times, and β is the baseline to which the data are asymptotic. (For the LL method, T1 in Eq. [14] should be replaced by $T1_{\text{eff}}$, given by Eq. [10].)

If the tip angles used in the multipoint sequence were perfectly known, a two-parameter fit (18–20) over the variables T1 and DR would be sufficient. Nonideal tip angles cause a shift in the baseline of the data. Since there is usually some uncertainty

in the exact tip angles employed, it is therefore often preferable to perform a three-parameter fit (1-4) over the variables T1, DR, and the baseline β . As the number of variables to be fitted increases, the error propagated into the T1 estimate due to random noise increases. However, high-field MRI units can provide data with an extremely high signal relative to random noise (SNR). The limit to the accuracy of relaxation time estimation is therefore likely to arise from systematic errors such as imperfect tip angles, rather than from the propagation of random noise. We note that two point ratio methods used in T1 estimation are highly susceptible to systematic errors. In this work, we have therefore considered the propagation of errors through a three-parameter fit of multipoint T1 relaxation data.

In the case of the ST method, mistuning of the two initial pulses (nominally equal to 90°) only affects DR, and a two-parameter fit over T1 and DR will not produce systematic errors in the T1 estimate, assuming there is no extra source of baseline offset. We have therefore considered a two-parameter fit to the ST multipoint data, in addition to a three-parameter fit.

Finally, it should be noted that, in some sequences, a three-parameter fit does not account for mistuning of every pulse. In the IR sequence, mistuning of the 90° pulse is not explicitly modeled by a three-parameter fit. However, the effect on the form of the fitting equation due to a mistuned 90° pulse is quite negligible under normal conditions, specifically whenever the repetition time $TR > T1$ (2, 4). In the LL method, it is impossible to distinguish the effect of the limited flip angle pulses from a relaxation effect. The LL method can therefore measure only an effective T1, given by Eq. [10]. This means that an error in our knowledge of α must always propagate into the T1 estimate, since α cannot be independently modeled in the least-squares fitting equation. We can rearrange Eq. [10] to give T1 in terms of α and calculate to first order the error propagated into the T1 estimate, $\delta T1 = (dT1/d\alpha)\delta\alpha$. As $\alpha \rightarrow 0$, the fractional error in T1, $\delta T1/T1$, also tends to zero, and for reasonably small α , this fractional error remains less than the fractional error in α . The ST method suffers from the same problem. Errors in the tuning of the limited flip angles will inevitably propagate errors into the T1 estimates, in essentially the same way as that in the LL method.

RESULTS

We have optimized each pulse sequence over the available pulse sequence parameters, with the restrictions already discussed. The optimization was performed by maximizing the figure of merit Γ , defined by Eq. [4], using the expressions for DR and T_{seq} given in Table 1. The calculation of the noise propagation factor b was performed using the expression given in the Appendix.

We have considered all timing parameters to be normalized with respect to a T1 equal to 1 s. Since we restrict our analysis to linear sampling of the T1 relaxation curve, with $t_1 = 0$, the sampling times $\{t_i\}$ can be characterized by the number of data points N , and the final sampling time t_N . Optimal values for these two parameters must be found for each of the four multipoint methods. The efficiency Γ of the IR method also depends on the repetition time TR. For any pair of values N and t_N , the optimal TR was found to be equal to t_N . This is to be expected, since only the T_{seq} term in the expression for Γ depends on TR, and this term must be minimized.

(TR cannot be less than t_N .) The efficiency of the ST method depends on the waiting time W . However, the dependence is not strong, with Γ broadly maximized around $W/T1 = 3$, and only dropping off noticeably when $W/T1 < 2$. The weak dependence is due to the competing influences of DR and T_{seq} on Γ , and the fact that both terms become larger as W increases.

In the case of the LL method, Γ also depends on the limited flip angle α . We have found that the optimal value of α depends strongly on N , as shown in Fig. 2. For a small number of data points, the optimal value of α is fairly large, so that a large component of magnetization is tipped into the transverse plane. As N increases, α must be reduced. This can be understood in terms of the effective T1, $T1_{\text{eff}}$, given by Eq. [10]. $T1_{\text{eff}}$ is always less than T1 (see Fig. 1d) and the effect of large values of both α and N is to make $T1_{\text{eff}}$ even shorter. Most of the data points therefore sample the baseline of the $T1_{\text{eff}}$ relaxation curve, causing the noise propagation term b to increase. The limited flip angle must therefore be reduced as N increases, at the expense of some loss in DR.

In Fig. 3, we show the dependence of Γ on the sampling parameters N and t_N . For the IR method, the results are shown with $TR = t_N$, for the ST method, $W/T1 = 3$, and for the LL method, the optimal α is found for each value of N using Fig. 2. The contour plots of Fig. 3 have a similar appearance for all four methods, although the maximum values of Γ differ considerably, as shown in Table 2. All multipoint methods display a peak efficiency at $t_N/T1$ between 3 and 4.5. For shorter t_N , it becomes difficult to estimate the baseline needed in a three-parameter fit to the T1 data, and the noise propagation term b therefore increases, causing a reduction in Γ . For higher values of t_N , the increase in sequence time T_{seq} causes Γ to drop again.

An optimal value of N between 5 and 8 exists for all multipoint methods. For smaller values of N , the number of degrees of freedom becomes too poor for a good estimate of T1 using a three-parameter fit, and Γ is reduced by an increase in b . For higher values of N , the efficiency drops off very slowly. The effect of increasing N is almost equivalent to additional signal averaging (1, 2, 4, 21); i.e., b is approximately proportional to $N^{-1/2}$. In the case of the recovery methods (IR and SR), a balance exists between a reduction in b and an increase in T_{seq} as N increases. In the case of

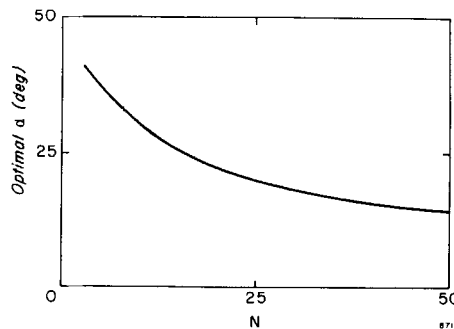


FIG. 2. Optimal limited flip angle α as a function of the number of data points N , collected along a T1 relaxation curve using the LL method.

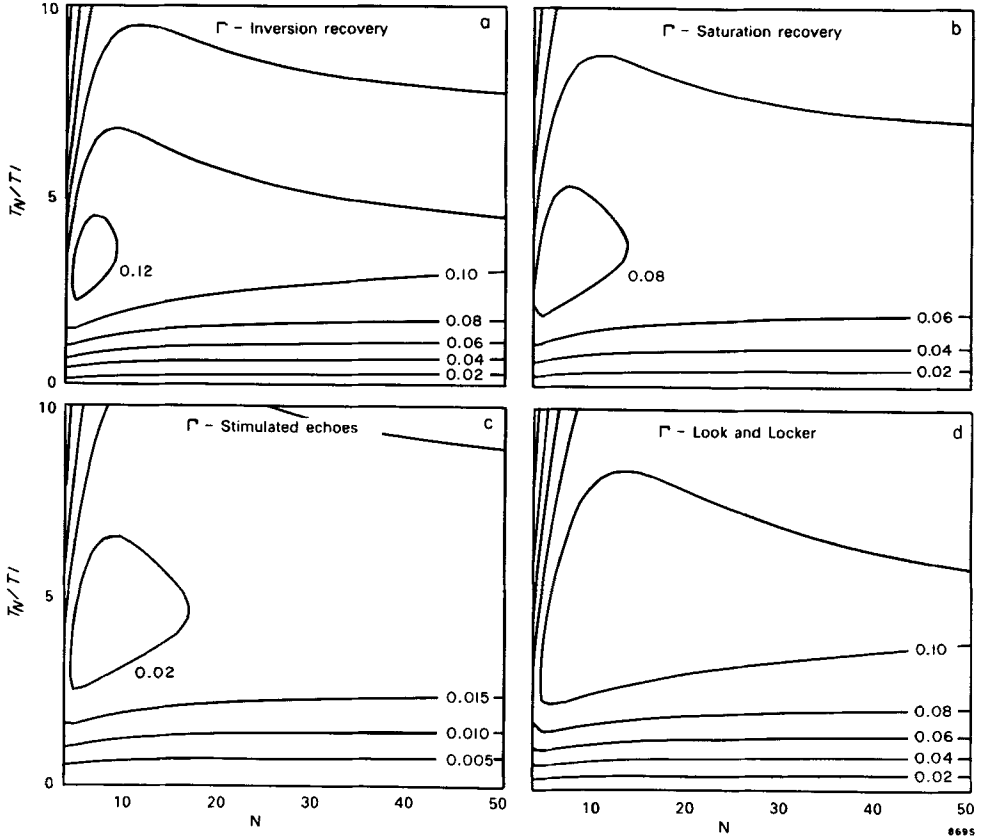


FIG. 3. Contours of relative efficiency Γ plotted as a function of sampling parameters N (number of data points) and $t_N/T1$ (t_N is the time of the last data point from the start of the T1 recovery curve). (a) IR method with $TR = t_N$, (b) SR method, (c) ST method with $W/T1 = 3$, (d) LL method with optimal $\alpha(N)$ taken from Fig. 2.

the “one-shot” methods (ST and LL), a similar balance exists between b and DR, which is also approximately proportional to $N^{-1/2}$. Therefore, the measurement of a large N , which enables a check for multiexponentiality, has little effect on the efficiency of any of the methods, but directly increases the minimum exam time of the recovery methods.

The optimized efficiencies of the four multipoint methods are given in Table 2. We note that the optimized efficiencies assume that our a priori estimate of T1 is correct, since the optimal choice of t_N depends on T1. The efficiency of each method in the case of a poorly “targeted” T1 estimate can be considered by moving away from the optimal value of t_N . The contour plots in Fig. 3 show a similar dependence of Γ on t_N for all four methods; i.e., all methods show essentially the same behavior as a function of T1 “targeting.” We are therefore justified in comparing the methods on the basis of their optimized efficiencies.

Of the recovery methods, the IR method is clearly superior to the SR method, due to a better dynamic range. Of the one-shot methods, the LL method is superior to the

TABLE 2
Optimized Sequence Parameters and Relative Efficiencies
of the Multipoint T1 Methods

	Optimized seq. parameters		DR	$T_{\text{seq}}/T1$	b	Relative efficiency Γ
	N	$t_N/T1$				
IR	5	3	2.00	15.0	4.0	0.13
SR	5	3	1.00	7.5	4.0	0.09
ST	6 (3)	4 (1.3)	0.19 (0.27)	7.0 (4.3)	3.3 (2.3)	0.02 (0.06) ^a
LL	8	4.5	0.84	4.5	3.5	0.12

^a Two-parameter fit.

ST method, even when the latter method is analyzed for a two-parameter fitting procedure (to allow for the fact that imperfect tip angles in an ST pulse sequence do not require a three-parameter model). The ST method suffers from a very poor DR and a sequence time T_{seq} that is longer than that of the LL method. Neither of these results is very surprising. What is of interest is that the best one-shot method (LL) has an efficiency that is almost equal to that of the best recovery method (IR). The importance of this result for T1 imaging is addressed in the next section.

DISCUSSION

Multipoint determinations of T1 relaxation times are useful for two reasons. They enable a three-parameter fit to reduce the systematic errors arising from a lack of knowledge of the precise tip angles. Multipoint data also enable the monoexponentiality of the data to be checked, which is important in MR imaging, where partial volume effects are often to be expected.

If multipoint recovery methods (IR and SR) are used for T1 mapping of a 256×128 image, the minimum exam time (i.e., with one average) can be prohibitively long. In such methods, it is impossible to trade off T1 image SNR in order to reduce the exam time, unless the number of pixels in the phase encode direction are reduced. These methods are therefore intrinsically slow. Such a trade-off is highly desirable for two reasons. First, the SNR increases only slowly as a function of exam time ($\text{SNR} \propto T_{\text{exam}}^{1/2}$). Second, with the availability of high-field MRI units, the accuracy of relaxation time measurements is likely to be limited by systematic errors that cannot be averaged out; i.e., a threshold SNR exists, above which no improvement in T1 accuracy can be expected.

If the field of view in the phase encode direction is decreased (keeping resolution fixed), the recovery methods become more practicable. Hence, they have always been the preferred method for spectrometer studies of T1 relaxation. For high-resolution images over a large field of view as in conventional imaging, a one-shot method may be preferred, since the reduction in sequence time T_{seq} does enable the SNR to be

traded for a reduction in exam time (by reducing N_{ex}). We have shown that the ST method suffers from a poor "efficiency" compared to the IR method; i.e., for a given exam time, the ST method produces a markedly inferior T1 image SNR. It is not surprising, therefore, that this one-shot method has not become a routine method of T1 imaging.

The LL method can be viewed as a modification of the limited flip angle, short repetition time sequence used in rapid imaging (22, 23), with essentially the same advantages and disadvantages. A possible disadvantage is its susceptibility to static field inhomogeneities, since an echo signal must be generated after the α pulse by a read gradient reversal instead of a 180° refocusing pulse. However, the exam time required to collect multipoint data across a 256×128 image is relatively short. We have shown that the LL method has an efficiency that is essentially equal to that of the IR method. There is therefore no intrinsic sacrifice in T1 image SNR, as a result of using the LL method to reduce the minimum exam time. The Look and Locker method would therefore appear to be the method of choice for T1 imaging.

APPENDIX

Statistical analysis of a least-squares fitting procedure yields the so-called error matrix $B = A^{-1}$, with the jk th element of matrix A , a_{jk} , given by

$$a_{jk} = \sum_{i=1}^N \frac{\partial S_i}{\partial X_j} \bigg|_{t_i} \frac{\partial S_i}{\partial X_k} \bigg|_{t_i}, \quad [\text{A1}]$$

where

$$S_i = \text{DR} \exp(-t_i/T1) + \beta. \quad [\text{A2}]$$

We consider a three-parameter fit over the variables $X_1 \equiv T1$, $X_2 \equiv \text{DR}$, and $X_3 \equiv \beta$. The elements of matrix A can all be conveniently expressed in terms of the summation

$$c_{mn} = \sum_{i=1}^N (t_i/T1)^m \exp(-nt_i/T1); \quad m, n = 0, 1, \text{ or } 2 \quad [\text{A3}]$$

as follows:

$$\begin{aligned} a_{11} &= (\text{DR}/T1)^2 c_{22} & a_{22} &= c_{02} & a_{33} &= c_{00} \\ a_{12} &= a_{21} = (\text{DR}/T1) c_{12} & a_{23} &= a_{32} = c_{01} & a_{13} &= a_{31} = (\text{DR}/T1) c_{11}. \end{aligned} \quad [\text{A4}]$$

Inverting matrix A gives the first element of the error matrix,

$$B_{11} = \frac{a_{22}a_{33} - a_{23}^2}{a_{11}a_{22}a_{33} + 2a_{12}a_{23}a_{13} - a_{12}^2a_{33} - a_{23}^2a_{11} - a_{13}^2a_{22}}, \quad [\text{A5}]$$

which can be expressed as

$$B_{11} = (T1/\text{DR})^2 b^2 \quad [\text{A6}]$$

with

$$b = \left(\frac{c_{02}c_{00} - c_{01}^2}{c_{22}c_{02}c_{00} + 2c_{12}c_{01}c_{11} - c_{12}^2c_{00} - c_{01}^2c_{22} - c_{11}^2c_{02}} \right)^{1/2}. \quad [\text{A7}]$$

In the case of the LL method, the variable T_1 in the exponential term of Eq. [A3] should be replaced by an effective T_1 , given by Eq. [10]. The dimensionless noise propagation term b is therefore dependent on the sampling times $\{t_i/T_1\}$ and also on the limited flip angle α for the LL method.

ACKNOWLEDGMENTS

Helpful discussions with E. R. McVeigh are gratefully acknowledged. Financial support for this work was received from the Medical Research Council of Canada, the National Cancer Institute of Canada, and General Electric Medical Systems of Canada. A. P. Crawley was supported by a University of Toronto Open Doctoral Fellowship.

REFERENCES

1. G. H. WEISS AND J. A. FERRETTI, *J. Magn. Reson.* **61**, 490 (1985).
2. G. H. WEISS AND J. A. FERRETTI, *J. Magn. Reson.* **61**, 499 (1985).
3. J. KOWALEWSKI, G. C. LEVY, L. F. JOHNSON, AND L. PALMER, *J. Magn. Reson.* **26**, 533 (1977).
4. J. GRANOT, *J. Magn. Reson.* **53**, 386 (1983).
5. R. M. KROEKER AND R. M. HENKELMAN, *J. Magn. Reson.* **69**, 218 (1986).
6. A. HAASE AND J. FRAHM, *J. Magn. Reson.* **65**, 481 (1985).
7. T. H. MARECI, W. SATTIN, AND K. N. SCOTT, *J. Magn. Reson.* **67**, 55 (1986).
8. D. C. LOOK AND D. R. LOCKER, *Rev. Sci. Instrum.* **41**, 250 (1970).
9. R. GRAUMANN, M. DEIMLING, T. HEILMANN, AND A. OPPELT, "Society of Magnetic Resonance in Medicine Fifth Annual Meeting, Montreal, 1986," p. 922. [Book of Abstracts]
10. W. H. HINSON, W. T. SOBOL, P. R. MORAN, AND D. A. SALONER, *Magn. Reson. Imaging* **5**(S1), 103 (1987).
11. W. T. SOBOL, W. H. HINSON, P. R. MORAN, AND D. A. SALONER, *Magn. Reson. Imaging* **5**(S1), 148 (1987).
12. M. O'DONNELL, J. C. GORE, AND W. J. ADAMS, *Med. Phys.* **13**, 182 (1986).
13. P. R. BEVINGTON, "Data Reduction and Error Analysis for the Physical Sciences," McGraw-Hill, New York, 1969.
14. W. A. EDELSTEIN, G. H. GLOVER, C. J. HARDY, AND R. W. REDINGTON, *Magn. Reson. Med.* **3**, 604 (1986).
15. J. GRANOT, *J. Magn. Reson.* **66**, 197 (1986).
16. R. K. GUPTA, J. A. FERRETTI, E. D. BECKER, AND G. H. WEISS, *J. Magn. Reson.* **38**, 447 (1980).
17. R. KAPTEIN, K. DIJKSTRA, AND C. E. TARR, *J. Magn. Reson.* **24**, 295 (1976).
18. G. H. WEISS, R. K. GUPTA, J. A. FERRETTI, AND E. D. BECKER, *J. Magn. Reson.* **37**, 369 (1980).
19. E. D. BECKER, J. A. FERRETTI, R. K. GUPTA, AND G. H. WEISS, *J. Magn. Reson.* **37**, 381 (1980).
20. R. J. KURLAND, *Magn. Reson. Med.* **2**, 136 (1985).
21. R. K. HARRIS AND R. H. NEWMAN, *J. Magn. Reson.* **24**, 449 (1976).
22. P. VAN DER MEULEN, J. P. GROEN, AND J. J. M. CUPPEN, *Magn. Reson. Imaging* **3**, 297 (1985).
23. A. HAASE, J. FRAHM, D. MATTHAEI, W. HANICKE, AND K. D. MERBOLDT, *J. Magn. Reson.* **67**, 258 (1986).